

OPEN ACCESS

EDITED BY

Aamir Ahmad,
University of Alabama at Birmingham,
United States

REVIEWED BY

Alex C. Kornke,
University of York, United Kingdom
Gerald Schwan,
University of Texas Southwestern
Medical Center, United States

*CORRESPONDENCE

Rui Xu
840420892@qq.com
Tao Ye
ye_tao@fudan.edu.cn

SPECIALTY SECTION

This article was submitted to
Molecular and Cellular Oncology,
a section of the journal
Frontiers in Oncology

RECEIVED 08 July 2022

ACCEPTED 09 August 2022

PUBLISHED 05 September 2022

CITATION

Zhang H, Xu XZ, Xu R and Ye T (2022)
Drug repurposing of ivermectin
abrogates neutrophil extracellular
traps and prevents melanoma
metastasis.
Front. Oncol. 12:989167.
doi: 10.3389/fonc.2022.989167

COPYRIGHT

© 2022 Zhang, Xu, Xu and Ye. This is an
open-access article distributed under
the terms of the [Creative Commons
Attribution License \(CC BY\)](https://creativecommons.org/licenses/by/4.0/). The use,
distribution or reproduction in other
forums is permitted, provided the
original author(s) and the copyright
owner(s) are credited and that the
original publication in this journal is
cited, in accordance with accepted
academic practice. No use,
distribution or reproduction is
permitted which does not comply with
these terms.

Drug repurposing of ivermectin abrogates neutrophil extracellular traps and prevents melanoma metastasis

Hongjun Zhang¹, XiaoZhu Xu², Rui Xu^{3*} and Tao Ye^{4,5*}

¹Department of Ophthalmology, Minhang Branch, Zhongshan Hospital, Fudan University, Shanghai, China, ²Department of Quality Arbitration, Shanghai Institute of Biological Products, Shanghai, China, ³Division of Rheumatology, Huashan Hospital, Fudan University, Shanghai, China, ⁴Department of Oncology, Minhang Branch, Zhongshan Hospital, Fudan University, Shanghai, China, ⁵Key Laboratory of Whole-Period Monitoring and Precise Intervention of Digestive Cancer (SMHC), Minhang Hospital & AHS, Fudan University, Shanghai, China

Neutrophil extracellular traps (NETs) have recently been identified to play a crucial role in cancer metastasis. However, the therapeutic target in NETs of melanoma cancer metastasis is still unknown. In this work, we screened a collection of 231 small molecule compounds. We identified ivermectin (IVM), a widely used antiparasitic drug, significantly inhibits neutrophil extracellular traps (NETs) formation after cathepsin B (CTSB) treatment. In vivo, IVM treatment showed no effects of melanoma tumor growth, while the orthotopic melanoma to lung metastasis was significantly suppressed by IVM. Serum level of myeloperoxidase-DNA and neutrophil elastase-DNA were suppressed after IVM treatment. Tumor infiltrated myeloid-derived suppressor cells (MDSCs) were significantly suppressed while tumor infiltrated CD8+T cells in lung was increased after IVM treatment in mouse melanoma model. Mechanistically, IVM targeted a pyroptotic driving factor gasdermin D (GSDMD), and exhibited a Kd of 267.96 nM by microscale thermophoresis (MST) assay. Furthermore, the direct interaction of IVM and GSDMD significantly suppressed GSDMD oligomerization, which are essential for GSDMD-dependent NETs formation. In vitro, treatment with CTSB in bone marrow neutrophils significantly promotes NETs formation, and the release of extracellular DNA was significantly suppressed by IVM pretreatment. Collectively, our results reveal that with the regulation role of IVM in neutrophils and NETs, IVM may potentially be used as a viable therapeutic approach for the treatment of melanoma cancer metastasis.

KEYWORDS

melanoma, drug repositioning, ivermectin, metastasis, neutrophil extracellular traps

Introduction

Melanoma is the cancer of the skin's pigment cells that caused by abrupt ultraviolet UV radiation from artificial sources or natural sunlight (1, 2). The treatment of melanoma is developing rapidly, including complementary disease prevention and detection strategies. However, in recent decades, the incidence rate of melanoma in white people around the world has increased steadily (3). Although early melanoma is not fatal, it can be cured by surgery (4). The high incidence rate of postoperative melanoma is still manifested by adverse medical history, and the late stage is the difficulty (5). Metastasis of melanoma is regulated by primary tumor cell exfoliation, tumor inflow or expulsion from the blood circulation system, epidermal serum stromal transformation (EMT) and withdrawal of host immune monitoring (6). In recent years, tumor microenvironment (TME) plays an important role in tumor metastasis and helps tumor patients respond (7). New strategies of adaptive immunotherapy, such as antigen-4-related T lymphocyte cytotoxicity (CTLA-4) and programmable cytokine 1 (PD-1), have played an important role in improving the prognosis of melanoma cancer (7). However, the role of innate immune cells in melanoma, especially in cancer metastasis, is still unclear.

In the endogenous immune cells impregnated with TME (such as bone marrow suppressor cells, platelets, macrophages), neutrophils play an important role in the development and metastasis of cancer (8). One of the most important functions of neutrophils is to accept neutrophil extracellular traps (NETs), which is defined as a mechanism to protect neutrophils from bacterial infection (9). Among non-communicable diseases, including gout, diabetes, rheumatoid arthritis, and even 2019 coronary artery disease (10–13), network therapy has received special attention. Recently, people have paid a lot of attention and studied its role in tumor metastasis and immunological deviation (14). Neutrophil infiltration is often found in ulcerative melanoma, and neural stem cells are related to the development of tumor (15). In addition, retrospective metastasis of old neutrophils significantly enhanced melanoma (B16LS9) due to cancer cell metastasis through the NETs (16, 17). Therefore, in our study, we tested the presence of 231 natural small molecule compounds from the database of Drug Bank and found the formation of reticular structures in the primary level lung melanoma metastasis model in mice.

Cathepsin B (CTSB) belongs to the papain family of cysteine proteases from the lysosome and is crucial for a cellular process called lysosomal membrane permeabilization. The function of CTSB was to degrade components of the extracellular matrix, which contributes to the development and metastasis of tumors (18). CTSB is produced constitutively and was identified as a

housekeeping protein, and was highly upregulated in malignant tumors (19). Aberrant overexpression of CTSB has been reported in invasive and metastatic cancers including breast cancer, melanoma and colorectal cancer (20). In melanoma, serum level of CTSB were significantly elevated in melanoma patients and identified as a prognosis marker for melanoma mortality (21). Recently, cathepsin B and D are involved in carcinogenesis and constitute bypass loops of the renin-angiotensin system in neck metastatic malignant melanoma cancer (22). In our study, we investigated the precise mechanism of CTSB in melanoma metastatic by controlling NETs formation as well as for screening the suitable molecule to block the above mechanism.

Ivermectin (IVM) is a macrolide antiparasitic drug that consist with 16 membered rings derived from avermectin family members include selamectin, doramectin and moxidectin (23, 24). Currently, IVM is the most successful avermectin family drug and the discovery of the excellent efficacy of IVM against parasitic diseases won the 2015 Nobel Prize in Physiology or Medicine (25). Despite the strong effects on parasites and antiviral effects, a few relevant studies have identified the potential use of IVM as a new cancer treatment. IVM could significantly suppress the mitochondrial membrane potential and inhibit mitochondrial respiration and ATP production in renal carcinoma cells without affecting the normal kidney cells (26). In addition, the proliferation of breast tumor cell lines was significantly suppressed by IVM-dependent cell cycle arrest and apoptosis (27). Therefore, the mechanism of the inhibition of tumor proliferation and the way that IVM induces tumor programmed cell death provide a theoretical basis for the use of IVM as a potential anticancer drug. However, the effect of IVM on immune cells in the tumor microenvironment are not known.

In this study, we found that IVM significantly inhibited the transformation of melanoma. We also identified a new mechanism, namely the formation of IVM/GSDMD dependent network, and the recently discovered IVM reconstruction of the micro immune environment for lung tumors. We also explored the possibility of treatment in the context of melanoma metastasis to this pathway.

Materials and methods

Cell culture

Bone marrow neutrophils isolated from wide type (WT) mice. Cells were collected in D-Hank's buffer (1x) of bone marrow from tibias and femurs. Following red cell lysis by ACK, cells were centrifuged (2000 g, 25 min, room

temperature) in 62.5% percoll (GE Health care, 17089102) without braking. Neutrophils lay in the bottom of centrifugal tube. After removing supernatants, cells were washed by PBS. The purity of neutrophils was determined by flow cytometry. Cells were cultured in complete RPMI 1640 media (10% FBS, 0.05 mM 2-mercaptoethanol, 1 mM NEAA). B16F10 cells were cultured in complete DMEM media containing 10% FBS.

Murine models

C57BL/6 mice were purchased from Cyagen. All mice were maintained in pathogen-free facilities in a specific pathogen-free facility at Fudan University. Animal experiments used all female mice with 4-6 weeks. Animals were randomly allocated to experimental groups. All animal experiments were approved by the Institutional Animal Care and Use Committee of Fudan University. The maximal tumor measurements/volumes are in accordance with the IACUC.

NETs detection with sytox green

NETs formation was quantified using an approach previously described (28). Briefly, bone marrow neutrophils were plated in 96-well culture plate at 3×10^4 per well in RPMI 1640 medium supplemented with 0.5% heat-inactivated FCS and 0.5% BSA. After 8 hours of stimulation, 0.2 μ M Sytox green (MCE, HY-K1077) was added for 15 min. Fluorescence was quantified at excitation and emission wavelengths of 488 nm and 520 nm, respectively. Wells were set up in triplicate and the results averaged to obtain a single data point.

CCK8 analysis of cell viability

B16-F10 cells were seeded in 96 platform plates with 1×10^4 cells/well, after 24 h, treated with mentioned concentrations of DMSO or IVM for 48 h. Replaced the medium with fresh medium, add 10 μ l CCK8 solution, and detect the OD₄₅₀ value with a microplate reader after 2-4 h. Data were analyzed and normalized to DMSO control. Viability (%) = $[\text{OD}_{450} (\text{Cells treated with indicated concentration of drug in the presence of CCK8}) - \text{OD}_{450} (\text{Only medium})] / [\text{OD}_{450} (\text{Cells treated with DMSO in the presence of CCK8}) - \text{OD}_{450} (\text{Only medium})] \times 100$.

Flow cytometry analysis

For neutrophils, bone marrow cells were isolated from C57BL/6 mice after treated with DMSO, IVM (5 μ M) for 2 h,

washed cells 2 times with PBS, stained with LIVE/DEAD(APC-Cy7) and anti-Ly6G, anti-CD11b for 15 min at 4°C, then washed cells with PBS for 2 times, stained with DCFH-DA for 30 min at 37°C, washed cells with cold PBS for 2 times. BD LSRFortessa was used for data acquisition and FlowJo (Tree Star) was used for data analysis.

For lung FACS analysis, the methods were used as previously described (29). Lung was collected, minced and digested by 33.3 U/mL DNaseI (Sigma D4513) and 0.5mg/mL Collagenase IV (Sigma C5138) at 37°C for 1 h. To analyze immune cell in the lungs, cells were incubated with zombie in PBS at 4°C for 30 min in dark. Then, Fc blocking were performed with CD16/CD32 antibodies in FACS buffer (1x PBS with 0.5% FBS, 2 mM EDTA) at 4°C for 30 min in dark. The cells were suspended in FACS buffer with PE-anti-mouse CD8 (clone 53-6.7, Cat#100750), Bv421-anti-mouse CD4 (clone RM4-5, Cat#100544) antibodies APC-cy7-Rat anti-mouse Ly6G (clone 1A8, Cat#127626), APC-anti-mouse Ly6C (clone HK1.4, Cat#128008), Perpcy5.5-anti-mouse CD11b (clone M1/70, Cat#101212), 4°C for 30 min in dark. Flow cytometry was performed by BD Fortessa X20 (BD Biosciences) and Data were analyzed utilizing FlowJo software (Tree Star, Inc.).

In vivo mouse models

To test the effect of IVM on skin melanoma mouse model, B16F10 cells were washed three times with PBS, B16F10 cells (2×10^5) were subcutaneously injected into the dorsal part of mouse (aged 8-10 weeks). After 1 week, mice were randomly divided into two groups, each of 5 mice, and treated as follows: (i) normal diet plus oral administration of 0.5% carboxymethyl cellulose sodium (NaCMC) as control (Vehicle) every day; (ii) normal diet plus oral administration of 10 mgkg⁻¹ IVM every day. From day 7, tumor volume was measured every 3 days, and animal survival rate was recorded every day. Tumor volume was calculated as length \times width \times width \times 0.5. Mice with tumor size larger than 20 mm at the longest axis were euthanized for ethical consideration. To analyze effector function of tumor-infiltrating lymphocytes, mice were euthanized on day 21.

ELISA analysis of serum CTSB assay

The level of CTSB in the serum was quantified using the Cathepsin B. Human ELISA kit (Abcam) in accordance with the manufacture's protocol. The level of TGF- β , VEGF and MMP9 were analyzed using ELISA kit in accordance with the manufacture's protocol (Ray-Bio).

Confocal immunofluorescence imaging

Imaging was performed on a custom modified Olympus FV3000 Laser Scanning Microscope equipped with a $\times 60$ oil immersion lens. Briefly, bone marrow neutrophils were seeded in chambers and stimulated with Control (DMSO), IVM (5 μ M), CTSB (5 μ M), PMA (20 nM) for 2 h at 37°C. The cells were fixed with 4% paraformaldehyde (PFA) and 0.1% Triton X-100 for 1 h at 4°C, followed by 5% BSA blocking for 30 min at 37°C. The cells were gently washed three times with PBS and stained overnight with the indicated antibodies at 4°C. After three washes with PBS, the cells were incubated with the indicated secondary antibody for 1 h at 4°C, and gently washed three times with PBS before imaging. The images were analyzed by using Image J.

Real time-PCR

The RNA from the lung of indicated groups was extracted using TRIzol reagent (Invitrogen). Then 5 ng of mRNA were subjected to cDNA synthesis. RT-PCR was performed using SYBR Green Supermix (Toyobo). The sequences of the primers of the indicated genes are:

IL-1 β	F: 5'- AATGCCACCTTTTGACAGTGA- 3'	R: 5'- GTCCTCATCCTGGAAGTCC-3'
TNF- α	F: 5'- CGAGTGACAAGCCTGTAGCC- 3'	R: 5'- ACAAGGTACAACCCATCGGC-3'
IL-6	F: 5'- CACCTCACAAAGTCGAGGCT- 3'	R: 5'- CTGCAAGTGCATCATCGTGT- 3'
GAPDH	F: 5'- TGCACCACCAACTGCTTAGC- 3'	R: 5'- GGCATGGACTGTGGTCATGAG- 3'

Western blot

Cells were collected to lysis buffer in cell lysis buffer (CLB) supplemented with protease and phosphatase inhibitor cocktail (Topscience Co., Ltd.) after treated with IVM (5 μ M) or CTSB (5 μ M). The lysed protein was loaded on a 10% polyacrylamide gel for SDS-PAGE, then transferred to a PVDF membrane at 200 mA for 80 min. The membrane was blocked at room temperature in 5% BSA for 1 h, incubated at 4°C overnight with the following primary antibodies: IL-1 β (#12242S), GAPDH (#8884) from Cell Signaling Technology. GSDMD

(ab219800), cit H3 (ab5103) was purchased from abcam. Pro-caspase-3 (MA5-32027) was purchased from ThermoFisher SCIENTIFIC. The membrane was washed three times in the TBST and probed with secondary antibodies (Proteintech, China). Finally, the membrane was imaged by imaging system (Tanon, Shanghai, China).

Protein labeling and microscale thermophoresis analysis

The binding affinity of GSDMD and IVM was measured at 25°C in a binding buffer (PBS containing 0.05% Tween 20) by Microscale Thermophoresis using MONOLITH NT.115. 100 μ l His-GSDMD or His-Caspase-4 at a concentration of 160 nM was incubated with 100 μ l 100 nM RED-tris-NTA 2nd Generation dye in the dark for 30 min. After incubation, the labeled GSDMD or Caspase-4 was mixed 1:1 with IVM in a two-fold dilution series from 49 nM-150 μ M for the measurement. The samples were loaded into NanoTemper Monolith NT.115 glass capillaries and MST carried out using 40% MST power. K_d values were calculated using the mass action equation and NanoTemper software, the data were plotted by the GraphPad Software.

Compound screening assay

Bone marrow neutrophils were isolated from C57BL/6 mice and cultured in 10% FBS. Cells were pre-treated with murine granulocyte colony-stimulating factor (PeproTech) for 2 h at 5% CO₂ with 37°C. Neutrophils were preincubated with small molecular compounds (Topscience Co., Ltd.) for 2 h. Then, cells were stimulated with recombinant mouse active CTSB (R&D, Cat#2336-CY) for 24 h at 37°C. NETs were detected by ELISA after staining with the cell-permeable DNA dye Sytox Green.

Statistical analyses

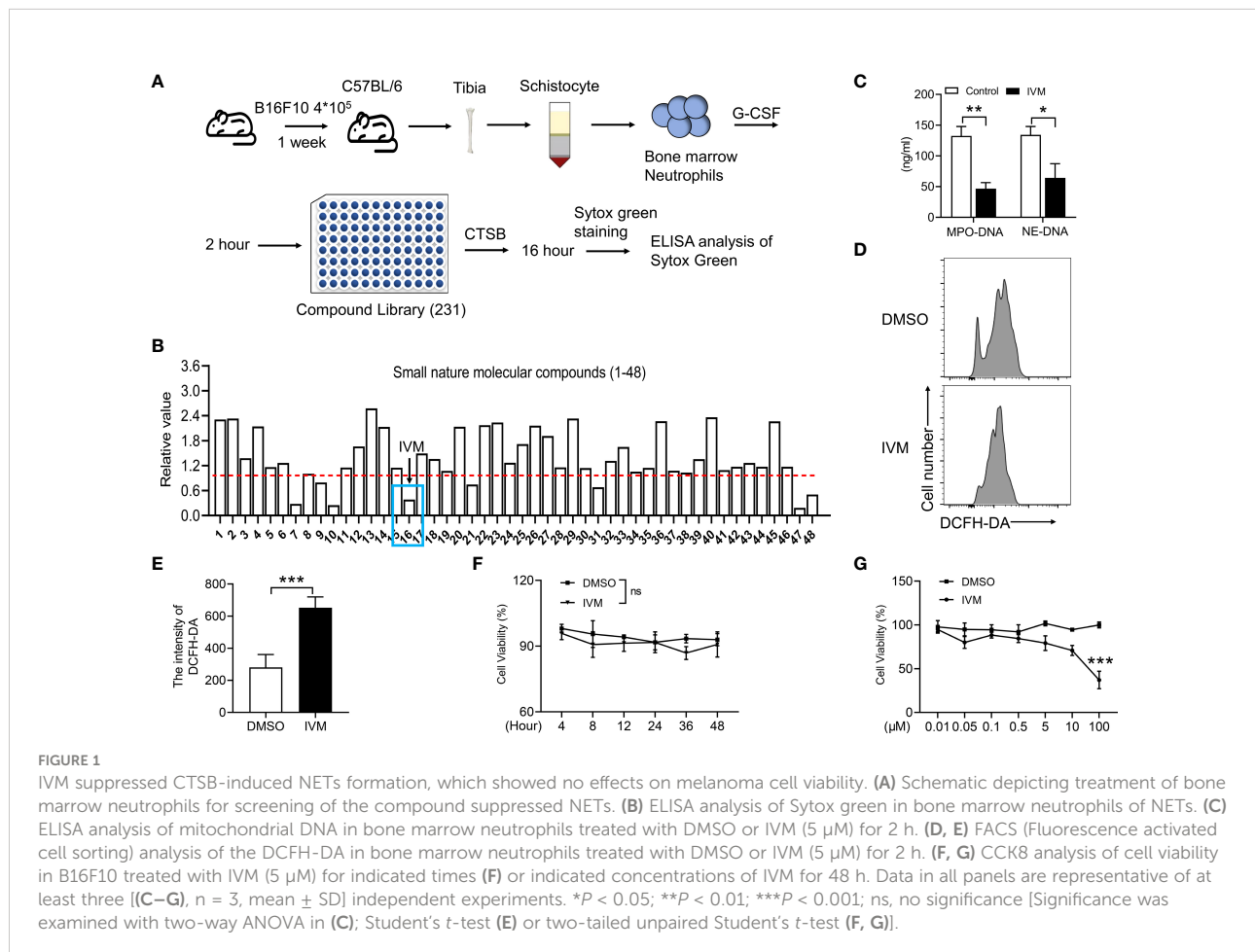
All statistical analyses were performed utilizing GraphPad Prism 7 (GraphPad Software). Statistical significance was calculated using unpaired Student's t-tests to compare the means of two groups, one-way analysis of variance (ANOVA) or two-way ANOVA to compare the means of three or more groups. All p values are two-tailed, and p values < 0.05 are considered significant (* p < 0.05, ** p < 0.01 and *** p < 0.001). The data are represented as mean \pm S.E.M. or the median with 10 and 90 percentiles.

Results

A screen of nature compound system revealed that cathepsin B-induced NETs formation was significantly suppressed by ivermectin

It is suggested that drug repositioning is a good strategy for reducing drug development time, lower costs and improve success rates. Drug repurposing are consisting of two strategies including activity-based drug repositioning and computational drug repositioning. Herein, we identified a screen system to detect small molecular compounds that suppressed NETs released after cathepsin B (CTSB) treatment. Bone marrow neutrophils were isolated from a mouse model of melanoma, cells were pretreated with granulocyte colony stimulating factor (G-CSF) for 2 hours. Then the cells were coated on the 96-plate at a density of 2×10^4 with indicated anti-cancer compounds for 48 h (Figure 1A). NETs were quantified by the intensity of Sytox

green (Figure 1B). The results showed the sixteenth compound, ivermectin (IVM), significantly suppressed NETs formation (Figure 1B). To further explore the role of IVM on NETs formation. Mitochondrial DNA detected by ELISA. CTSB-induced increased mitochondrial DNA was significantly suppressed by IVM (Figure 1C). In addition, several lines of evidence suggest that the formation of NETs are dependent on elevating intracellular reactive oxygen species (ROS) level (30). Our results showed a significant increase of DCFH-DA intensity of bone marrow neutrophils after IVM treatment (Figures 1D, E), indicating the role of IVM on ROS production in neutrophils. Furthermore, we detected the different times and concentration of IVM on the cell viability of melanoma cells. The results showed that $5 \mu\text{M}$ IVM showed no viability effect on B16F10 cells during 48 h (Figure 1F). And the viability of B16F10 was only suppressed after a high dosage treatment with IVM (Figure 1G). Thus, these findings indicated that IVM suppressed CTSB-induced NETs formation, which showed no effects on melanoma cell viability.



IVM significantly suppressed melanoma to lung metastasis in a B16F10 *in situ* mouse model

We next sought to explore the effect of IVM on melanoma tumor in a murine B16F10 model. We subcutaneously injected 2×10^5 B16F10 cells into each dorsal flanks of C57/BL mice. The mice were then divided into three groups: control mice; B16F10 mice + NaCMC; B16F10 with IVM (10 mg/kg) treatment through oral administration every other day during 14 days (Figure 2A). The tumor volume and body weight measurements of the indicated group were taken once 3 days. The results showed that tumor volume was not reduced after IVM treatment (Figures 2B, C). Surprisingly, the metastasis of B16F10 cells into the lung was significantly suppressed after IVM treatment (Figures 2D, E). We also detected the survival rate of ovary tumor xenograft mouse model, the survival rate of tumor mice was significantly reduced at 22 days, while the survival rate of tumor mice was still over 50% after 22 days (Figure 2F). The level of transforming growth factor (TGF- β), vascular endothelial growth factor (VEGF) and matrix metalloproteinase 9 (MMP9) were significantly increased in lung, while these pro-

metastatic factors were suppressed after IVM treatment (Figure 2G). To investigate the effect of IVM on immune response. The expression of pro-inflammatory cytokines in lung were detected. In the transcriptional level, cancer related cytokines including *IL-1 β* , *IL-6* and *TNF- α* were all reduced after IVM treatment (Figure 2H). We also detected the level of CTSB in serum from tumor mouse model. ELISA data showed the level of CTSB in serum was significantly increased after B16F10 cells injection (Figure 2I). Collectively, these data indicate that IVM suppressed the progression of melanoma cancer to lung metastasis.

IVM reshaped the tumor immune microenvironment in lung of melanoma mouse model

To further assess the effects of IVM in micro-immune environment in melanoma to lung metastasis. The immune cells in lung were detected by flow cytometry. Our results showed a significant increase of cell percentage of monocytes (CD11b⁺Ly6C⁺) and neutrophils (CD11b⁺Ly6G⁺) in lung of

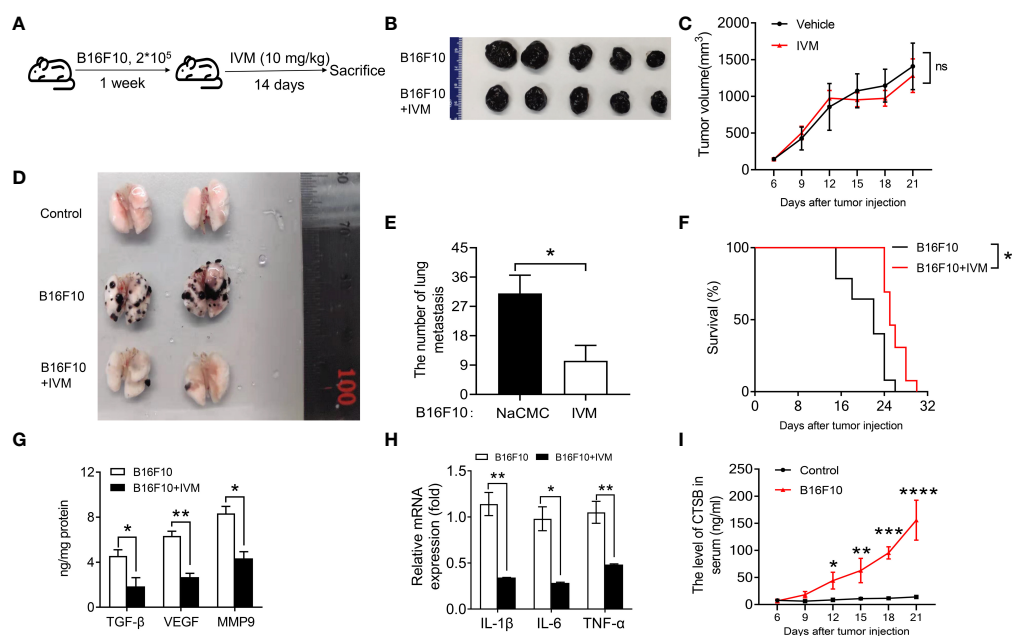


FIGURE 2

IVM significantly suppressed melanoma to lung metastasis in a B16F10 *in situ* mouse model. (A) Schematic depicting treatment of mouse B16F10-bearing melanoma mouse model. (B) Images of tumor from IVM (suspended in 0.5% NaCMC) and Vehicle (equal volume of 0.5% NaCMC)-treated mice after B16F10 melanoma inoculation at day 21. (C) Quantitative analysis of tumor volume in (B) ($n = 5$ mice per group). (D) Images of lung from control, B16F10 and B16F10+IVM groups. (E) Quantitative analysis of the number of lung metastasis in (D) ($n = 5$ mice per group). (F) Survival curves in IVM- and Vehicle-treated mice after B16F10 melanoma inoculation ($n = 5$ mice per group). (G) ELISA analysis of TGF- β , VEGF and MMP9 in the lung of mice from indicated groups. (H) Q-PCR analysis of *IL-1 β* , *IL-6* and *TNF- α* in the lung of mice from indicated groups. (I) ELISA analysis of CTSB in serum of mouse after B16F10 cells injection. Data in all panels are representative of at least three [(C, E–I), $n = 3$, mean \pm SD] independent experiments. * $P < 0.05$; ** $P < 0.01$; *** $P < 0.001$; **** $P < 0.0001$ [multiple t tests between the two groups in (E); two-way ANOVA in (C) and (I); two-way ANOVA in (G) and (H); log-rank (Mantel–Cox) test in (F)].

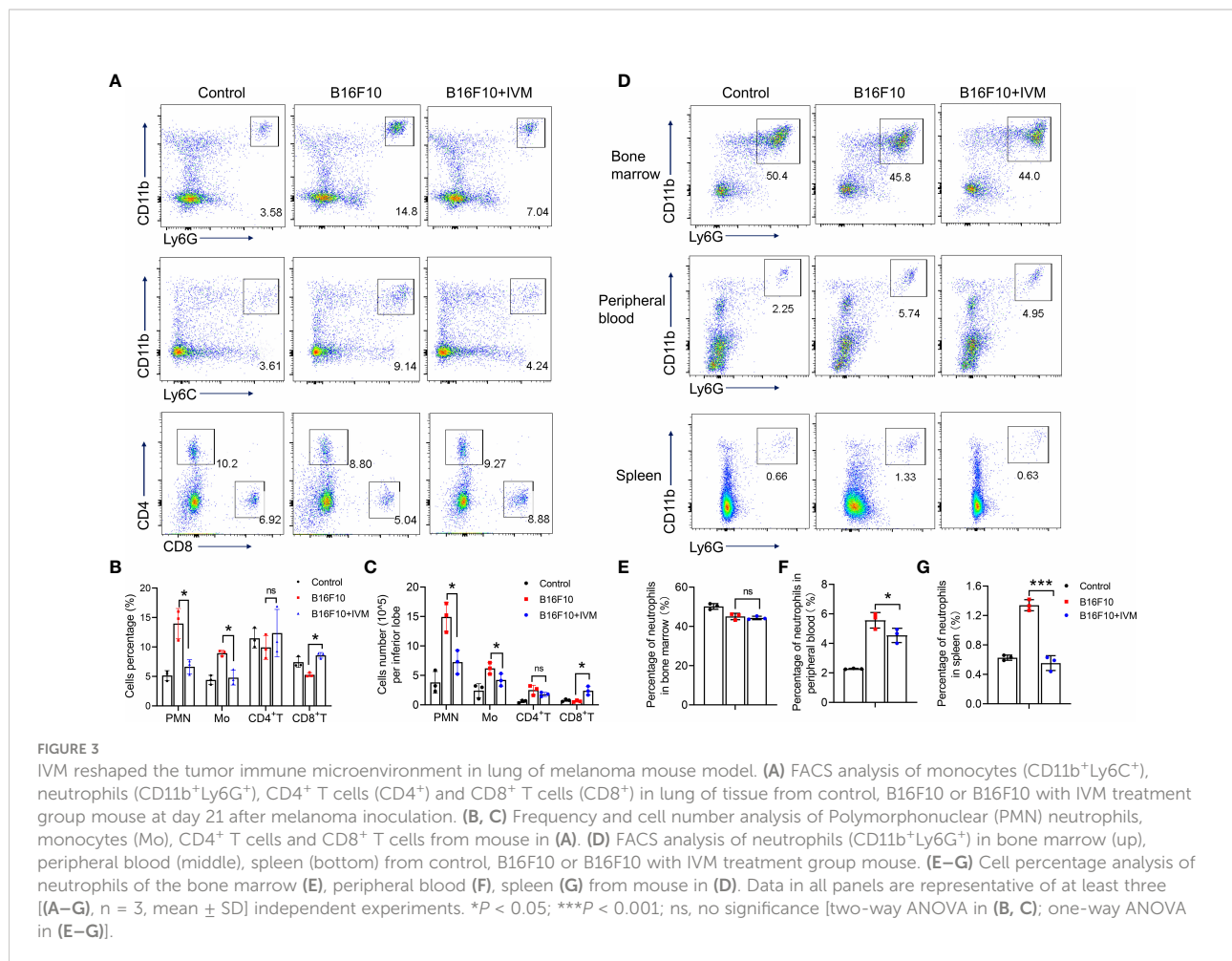
melanoma mice, while a reduced percentage of CD4⁺ and CD8⁺ T cells (Figure 3A). And the percentage of monocytes and neutrophils were reduced by IVM while an increased percentage of CD8⁺ T cells after IVM treatment (Figures 3A, B). Furthermore, by counting the absolute cell number, we also identified an increase cell number of neutrophils and monocytes in lung of melanoma mice, which were suppressed by IVM. Also, the reduced cell number of CD8⁺ T cells were increased after IVM treatment (Figure 3C).

To identified the precise role of neutrophils in melanoma tumor metastasis, we compared the percentage of neutrophils from bone marrow, peripheral blood and spleen. The percentage of bone marrow neutrophils in B16F10 mice was not increased compared with control (Figures 3D, E), indicating a no effect on hematopoiesis. The percentage of neutrophils were significantly increased in peripheral blood (Figures 3D, F) and spleen (Figures 3D, G), suggesting an increased migration of neutrophils from bone marrow. When treated with IVM, the percentage of neutrophils were suppressed in peripheral blood and spleen, while showed no effect on bone marrow neutrophils (Figures 3D–G). Taken together, these results demonstrate that

IVM suppressed metastasis by reshaping tumor immune microenvironment.

The formation of NETs in lung of melanoma mouse model was suppressed by IVM

To explore the role of NETs on melanoma metastasis, we detected NETs by Ly6G and cit-H3 (a biomarker of nuclear DNA decondensing and NETs) in lung section from B16F10 mice. The results of immunofluorescence showed an increased cit-H3 positive staining of Ly6G in lung of B16F10 mice, indicating the formation of NETs. And the increase of NETs was significantly suppressed after IVM treatment (Figures 4A, B). Notably, we used a previous report method to detect NETs in serum from B16F10 mice. The results showed the level of mitochondrial DNA was significantly reduced by IVM (Figure 4C). It is well known that the activation of CD8⁺ T cells in tumor micro-environment was significantly suppressed by myeloid derived suppressor cells (MDSC) (31). We further



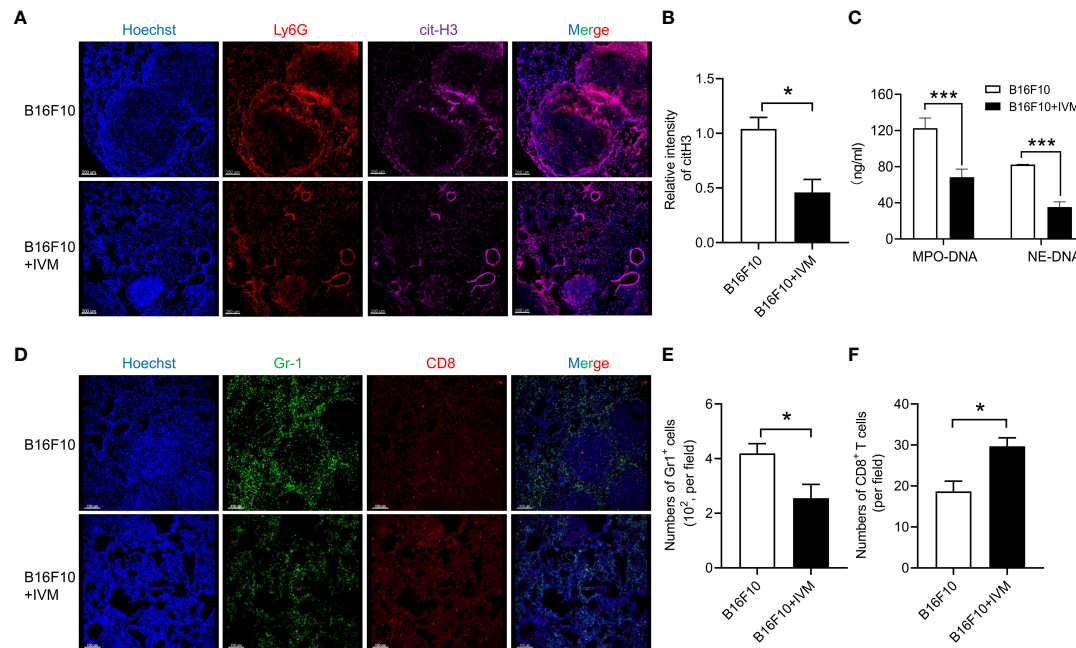


FIGURE 4

IVM suppressed NETs in melanoma metastasis. (A) Confocal analysis of Ly6G (red), cit-H3 (purple) in lung section from B16F10 or B16F10 with IVM treatment group mouse. (B) Quantitative analysis of relative intensity of cit-H3 ($n = 3$ field). Scale bars, 200 μm . (C) ELISA analysis of mitochondrial DNA in serum from B16F10 or B16F10 with IVM treatment group mouse. (D) Confocal analysis of Gr-1 (green), CD8 (red) in lung section from B16F10 melanoma bearing mouse. (E, F) Quantitative analysis of the number of Gr-1⁺ cells (E) and CD8⁺ T cells (F) ($n = 3$ field). Scale bars, 150 μm . Data in all panels are representative of at least three independent experiments [(B, C, E, F), $n = 3$, mean \pm SD]. * $P < 0.05$; *** $P < 0.001$ [multiple t tests between the two groups in (B), (E) and (F); two-way ANOVA in (C)].

investigated the quantity and distribution of MDSC (Gr-1) and CD8⁺ T cells in lung. As expected, immunofluorescence showed a reduced cell number of MDSC in metastatic tumor of lung after IVM treatment, while increased CD8⁺ T cells in lung metastatic tumors (Figures 4D–F). Taken together, these results demonstrate that IVM suppressed NETs and reshaped tumor immune microenvironment in melanoma metastasis.

CTSB-dependent NETs was significantly suppressed after IVM treatment

To further investigate the role of CTSB on NETs formation, we isolated bone marrow neutrophils from WT mice and treated with recombinant CTSB. Confocal analysis showed there is an increased release of NETs (as detected by Sytox green, cit-H3 and MPO positive staining) after 12 hours (Figure 5A). The treatment with PMA (20 nM) was showed as a positive control, which showed a highly increased NETs formation (Figure 5A). and the results showed nearly no spontaneous NTEs release after IVM treatment (Figures 5A, B). Furthermore, we also detected the level of NETs in cultured medium by mitochondrial DNA. The results showed an increased level of mitochondrial DNA in cultured medium after CTSB treatment, and this increase was

reduced after IVM treatment (Figure 5C). To further explore CTSB-induced NETs formation, scan electron microscopy (SEM) was used to identify extracellular mitochondrial DNA from bone marrow neutrophils. The results showed CTSB-induced NETs was significantly suppressed by IVM (Figures 5D, E). In addition, we detected the expression of CTSB through immunofluorescence. Confocal analysis showed that the expression of CTSB was significantly increased in lung of B16F10 mice (Figure 5F). Thus, our results showed IVM significantly suppressed CTSB-dependent NETs formation.

IVM directly interact with gasdermin D and promotes GSDMD oligomerization in neutrophils

We further explore the precise mechanism of IVM on NETs formation. Previous studies have suggested that the activation of Gasdermin D (GSDMD) is required for the generation of NETs (32, 33). However, whether GSDMD activation and GSDMD-dependent NETs is involved in melanoma metastasis are unknown. Bone marrow neutrophils were isolated from control and B16F10 mice. Western blot showed the detection of GSDMD-N terminal in B16F10 mice, but not control mice,

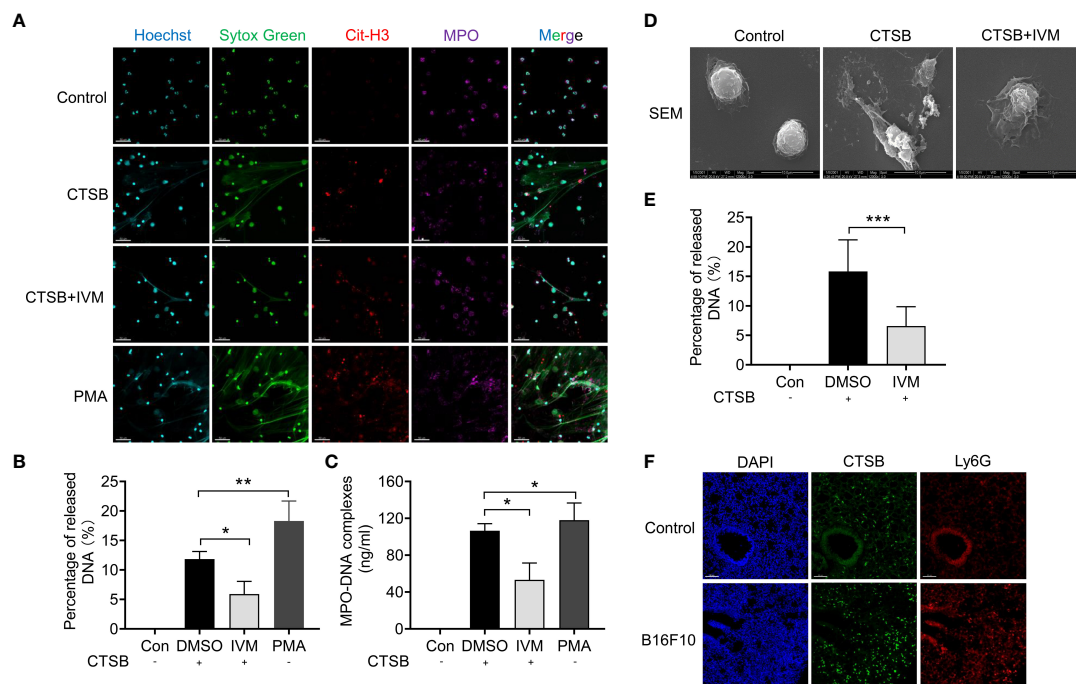


FIGURE 5

IVM significantly suppressed CTSB-dependent NETs formation. (A) Confocal analysis of Sytox Green (green), Cit-H3 (red) and MPO (purple) in bone marrow neutrophils from wide type mice and treated with recombinant CTSB, CTSB with IVM or PMA after 12 h. (B) Percentage of released mitochondrial DNA in (A) was quantified ($n = 3$ field). Scale bars, 50 μm . (C) Quantitative analysis of mitochondrial DNA in the cultured medium. (D) SEM (scan electron microscopy) and quantitative analysis (E) of extracellular mitochondrial DNA induced by CTSB in bone marrow neutrophils after treated with IVM. (F) Confocal analysis of the expression of CTSB (green) and Ly6G (red) in lung of B16F10 mice. Data in all panels are representative of at least three independent experiments. $*P < 0.05$; $**P < 0.01$; $***P < 0.001$ [one-way ANOVA in (B), (C) and (E)].

indicating the activation of GSDMD (Figure 6A). The expression of caspase-11 and cit-H3 was also increased compared with control mice (Figure 6A). IVM significantly suppressed the expression of cit-H3 while the expression of caspase-11 and GSDMD-N were not comparable with B16F10 mice (Figures 6A, B).

The oligomerization of GSDMD was required for its membrane pore formation (34). We next investigated the effect of IVM on GSDMD oligomerization in bone marrow neutrophils. Bone marrow neutrophils were isolated from WT mice and the cells were treated with CTSB for 12 h. Unchanged western blot showed that CTSB significantly promotes GSDMD oligomerization, while this increase was suppressed by IVM (Figures 6C, D). However, the cleavage of GSDMD was not reduced as GSDMD-N showed the same level after IVM treatment. This result suggests that IVM promotes GSDMD oligomerization but not cleavage (Figures 6E, F). We measured the binding dissociation constants (K_d) of purified GSDMD protein with IVM using microscale thermophoresis (MST). IVM interacted with purified GSDMD protein with a K_d of 267.96 nM (Figure 6G), while the interaction between IVM and GSDMD showed poor fitting (Figure 6H). Taken together, these results indicated that IVM directly interact with GSDMD to promotes

its oligomerization, and subsequent GSDMD-dependent NETs (Figure 7).

Discussion

In this study, we report that IVM, a generic drug approved by FDA, has antibacterial and anti-melanoma activities. We further identified the precise molecular target of GSDMD for IVM. The current research results show that IVM inhibits the formation of GSDMD dependent pores and the thermal swelling of cells, which significantly reduces the formation of reticular structures induced by CTSB, leading to melanoma metastasis.

Collectively, our research has found a new potential IVM target in the clinical treatment of melanoma.

Recently, drug repurposing has become a powerful tool for discovering and developing novel anticancer drug candidates (35, 36). Our *in vitro* screening system showed a broad-spectrum anti-parasitic compound IVM among 231 candidate small molecular compounds in the database of Drug Bank significantly reduced CTSB-induced NETs formation, with no effect on tumor cell viability. The prior investigation on repositioning drugs, such as mefloquine and albendazole have

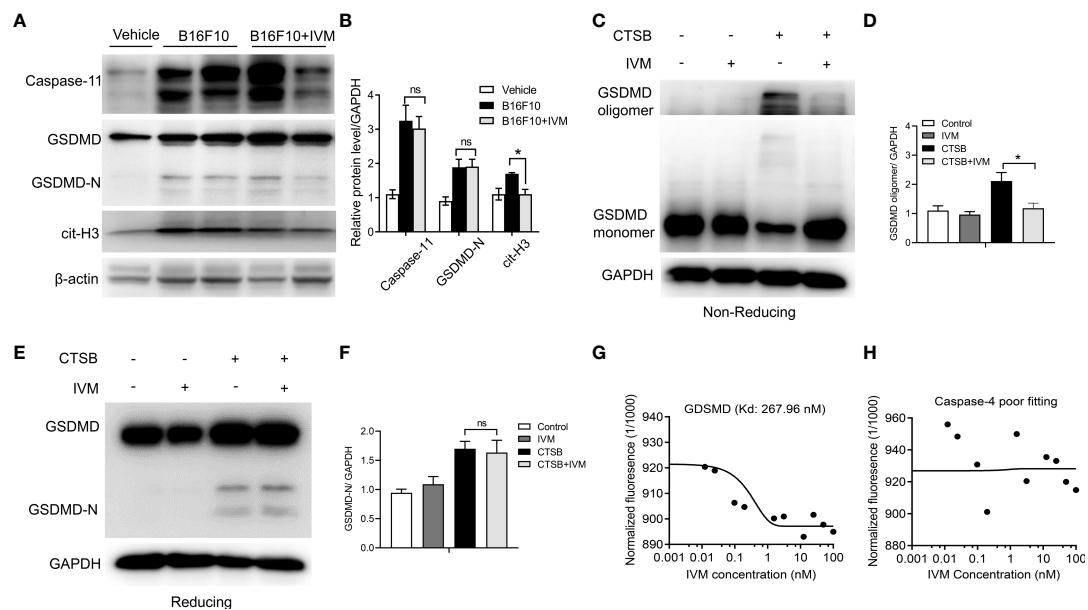


FIGURE 6

IVM directly interact with GDSMD to promote its oligomerization, and subsequent GSDMD-dependent NETs. (A) Western blot analysis of Caspase-11, GSDMD and cit-H3 expression in bone marrow neutrophils from control, B16F10 and B16F10 with IVM group. (B) Quantitative analysis of caspase-11, GSDMD-N and cit-H3 in (A). (C) Non-reducing western blot analysis of GSDMD in bone marrow neutrophils after CTSSB or CTSSB with IVM treatment. (D) Quantitative analysis of GSDMD oligomer. (E) Reducing western blot analysis of GSDMD in bone marrow neutrophils isolated from WT mice treated with CTSSB for 12 h followed by treatment with IVM for 2 h. (F) Quantitative analysis of GSDMD-N. (G) and (H) MST analysis determined the K_d of IVM towards His-GSDMD (267.96 nm) (G) or His-Caspase-4 (poor fitting) (H) labeled with RED-tris-NTA 2nd Generation dye. Concentration is reported in nanomolar. Data in all panels are representative of at least three independent experiments. * $P < 0.05$; ns, no significance [two-way ANOVA in (B), one-way ANOVA in (F)].

demonstrated to promote cancer treatment by targeting cell cycle arrest in melanoma cells (37, 38). IVM is widely used in both animals and human as an FDA-approved parasiticide (39). Except for its role as antiviral activity against several viruses such as coronaviruses, recent studies have revealed its role in various diseases, including sepsis, diabetes and human cancer disease (40–42). In tumor study, IVM has been identified to reverse the chemotherapeutic drugs resistance through EGFR pathway in colorectal and breast cancer (43). In addition, another study points to a repression of WNT- β -CATENIN/TCF transcriptional response by IVM and related macrocyclic lactones in human colon cancer (42). So further studies are required for us to investigate the role of IVM on melanoma cells in the pathogenesis of tumor metastasis.

Our immunofluorescent results showed IVM reshaped the tumor immune microenvironment with increased CD8⁺T cells and reduced MDSCs in lung of melanoma mouse model. The results suggest that IVM exhibit a strong potential for melanoma cancer to lung metastasis. Melanoma is recognized as one of the most immunogenic human cancer types that has a strong correlation between the infiltration of T cells in melanoma metastases (44, 45). In clinical phase III trial with 945 patients, the overall 5-year survival rate was 44% for anti-PD-1 (46). Therefore, a combination of anti-PD-1 antibody with IVM

should be added to further explore their effect on melanoma cell metastasis. Besides the role of CD8⁺T cells in melanoma metastasis, MDSCs were also found to be enriched and activated in the melanoma microenvironment. The reduced frequencies and cell number of MDSCs abrogate immunosuppressive functions that delay the tumor progression and prolong the survival both in animal models and in cancer patients (47, 48). So further studies are required to investigate the direct effect on IVM on CD8⁺T cells and MDSCs in melanoma metastasis.

Our molecular mechanism study identified IVM directly interact with GSDMD and promotes GSDMD oligomerization in bone marrow neutrophils. GSDMD is a pore forming protein that acts as a downstream molecular of inflammasome and non-canonical inflammasome (caspase-11). In innate immune cells such as macrophage, GSDMD is activated by the cleavage of canonical (NLRP3, AIM2, and caspase-1) or noncanonical pathway. Once cleaved, GSDMD can translocate to the plasma membrane to form pores and induce a lytic proinflammatory of cell death (49, 50). However, unlike macrophages, which undergo pyroptosis, the activation of canonical inflammasome in neutrophils facilitate NETosis. Recently, two studies have identified that the activation of gasdermin D (GSDMD) is required for the generation of NETs (32, 33). Secondly, although many studies have been focused on the regulation

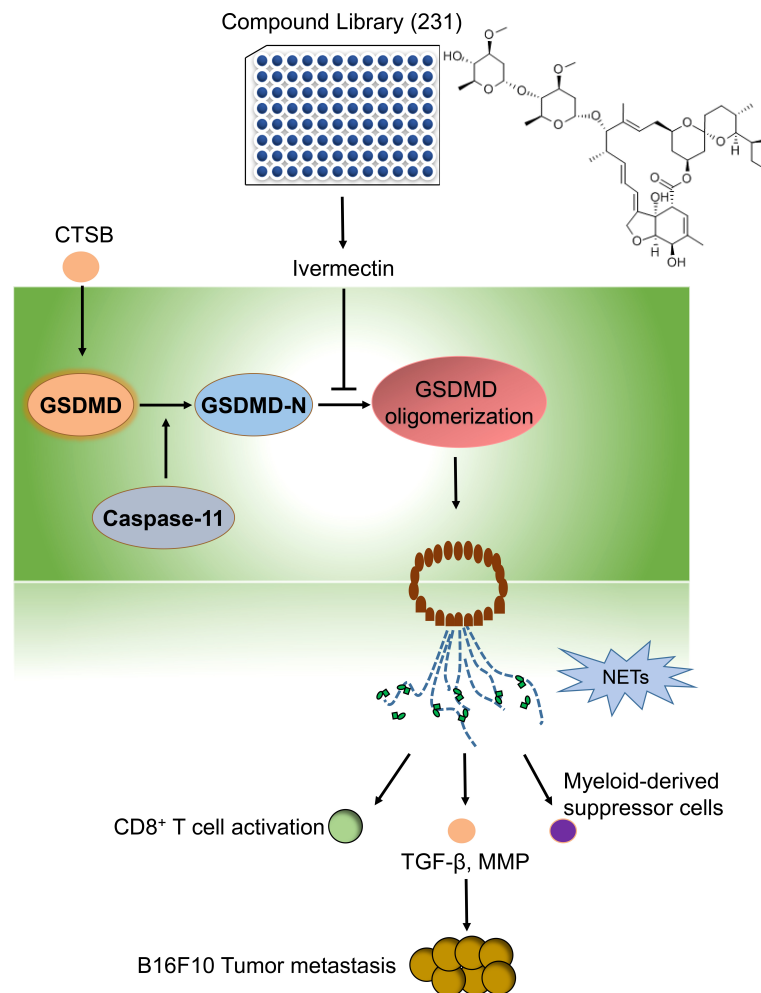


FIGURE 7

The graphic abstract in this study. By using a compound library, we identified a natural compound IVM, which significantly suppressed CTSB-induced NETs. The precise mechanism of IVM was targeting GSDMD and significantly suppressed GSDMD oligomerization. Thus IVM suppressed GSDMD-dependent NETs. The formation of NETs significantly promotes melanoma cancer metastasis through increasing TGF- β , MMP9 and myeloid-derived suppressor cells and suppressed CD8⁺T cells activation.

pathway for GSDMD cleavage (such caspase-8, caspase-3). Little is known for the regulation role of GSDMD pore formation on the plasma membrane. Our results further confirm a role of IVM on GSDMD oligomerization, which is essential for GSDMD pore formation (2, 51). However, our results showed no effect of GSDMD cleavage after IVM treatment. The upstream enzyme of GSDMD is caspase-1 and caspase-11, our results showed there is no comparable effect of caspase-11 after IVM treatment. Since caspase-1 was not required for GSDMD-dependent NETs (32). We did not detect the expression of caspase-1, especially in neutrophils, except for caspase-1 and caspase-11, the resident granzyme in neutrophil can also cleave GSDMD including elastase and cathepsin G (52, 53). So, our study should also investigate the effect of IVM on elastase and cathepsin G.

The results of immunofluorescence and scanning electron microscope showed the release of NETs were significantly increased after CTSB treatment. Indicating the role of CTSB on NETs formation. Except for the role of CTSB on NETs, it has been identified that cathepsin protease is essential for melanoma progression (54). Intracellular cathepsins cleave proteins while extracellular cathepsins degrade type I collagen and active pro-invasive proteases in the tumor microenvironment, which promotes tumor metastasis (55). CTSB cleaves in the non-helical telopeptide extensions of collagens (56). The secretion of CTSB is significantly increased in cancer cells and are active and stable in acidic environments and neutral acidity (57). A study showed that Abl/Arg promoted CTSB secretion through controlling the transcription factors with epithelial

mesenchymal transition (EMT), invasion and therapeutic resistance in melanoma cells (58). Except for the role of CTSB on tumor cells, there are some reports that CTSB interacting with NLRP3 and to subsequent caspase-1 activation in macrophages (59). In our study, further investigations are thus needed to explore the role of CTSB on other cells.

It has been identified that inflammatory cytokines and growth factors play a crucial role in tumor growth and tumor microenvironment. The qPCR results showed that the level of proinflammatory cytokines including IL-1 β , IL-6 and TNF- α were significantly reduced in lung of B16F10 mice after IVM treatment. Melanoma cells often express variable levels of IL-1 β and IL-6, which plays an important role of cell proliferation and melanoma progression (60). Also, the level of TGF- β , VEGF and MMP9 were reduced after IVM treatment. TGF- β is a multifunctional cytokine belong to the transforming growth factor superfamily, the key function is to regulate the inflammatory process. In melanoma, TGF- β is considered a marker of metastatic spreading (61). In addition, recent studies suggested that TNF- α and metalloproteases were key players in melanoma cells aggressiveness (62, 63). So further studies are required to investigate the precise effect of IVM in these pro-inflammatory cytokines and growth factors as secreted from B16F10 melanoma cells.

Overall, the data from this study suggest the role of IVM in the formation of CTSB induced reticular formation when melanoma metastasizes to the lungs. We found that CTSB secreted by tumor significantly promoted the activation of neutral caspase-11/GSDMD cells IVM directed at SDMX has greatly inhibited SDMX oligarchy and the subsequent GSMX core network. As the clinical needs of patients with melanoma have not been met, it is necessary to further explore the feasibility of this drug as a treatment for melanoma metastasis.

Date availability statement

The original contributions presented in the study are included in the article/supplementary material. Further inquiries can be directed to the corresponding authors.

References

1. Arnold M, Singh D, Laversanne M, Vignat J, Vaccarella S, Meheus F, et al. Global burden of cutaneous melanoma in 2020 and projections to 2040. *JAMA Dermatol* (2022) 158(5):495–503. doi: 10.1001/jamadermatol.2022.0160
2. Evavold CL, Hafner-Bratkovic I, Devant P, D'Andrea JM, Ngwa EM, Borsic E, et al. Control of gasdermin d oligomerization and pyroptosis by the regulator-Rag-mTORC1 pathway. *Cell* (2021) 184:4495–511.e4419. doi: 10.1016/j.cell.2021.06.028
3. Che G, Huang B, Xie Z, Zhao J, Yan Y, Wu J, et al. Trends in incidence and survival in patients with melanoma, 1974–2013. *Am J Cancer Res* (2019) 9(7):1396–414. doi: 2156-6976/ajcr0098195
4. Siegel RL, Miller KD, Fuchs HE, Jemal A. Cancer statistics, 2022. *CA Cancer J Clin* (2022) 72:7–33. doi: 10.3322/caac.21708
5. Chaffer CL, Weinberg RA. A perspective on cancer cell metastasis. *Science* (2011) 331:1559–64. doi: 10.1126/science.1203543
6. Hinshaw DC, Shevde LA. The tumor microenvironment innately modulates cancer progression. *Cancer Res* (2019) 79:4557–66. doi: 10.1158/0008-5472.CAN-18-3962
7. Luke JJ, Flaherty KT, Ribas A, Long GV. Targeted agents and immunotherapies: optimizing outcomes in melanoma. *Nat Rev Clin Oncol* (2017) 14:463–82. doi: 10.1038/nrclinonc.2017.43

Ethics statement

The animal study was reviewed and approved by All animal experiments were approved by the Institutional Animal Care and Use Committee of Fudan University. The maximal tumor measurements/volumes are in accordance with the IACUC.

Author contributions

HZ designed and performed experiments. XX helped with the experiments. RX and TY supervised the study and wrote the manuscript. All authors contributed to the article and approved the submitted version.

Funding

This work was funded by The National Key Research and Development Program of China (Grant No. 2019YFF021650210).

Conflict of interest

The authors declare that the research was conducted in the absence of any commercial or financial relationships that could be construed as a potential conflict of interest.

Publisher's note

All claims expressed in this article are solely those of the authors and do not necessarily represent those of their affiliated organizations, or those of the publisher, the editors and the reviewers. Any product that may be evaluated in this article, or claim that may be made by its manufacturer, is not guaranteed or endorsed by the publisher.

8. Uribe-Querol E, Rosales C. Neutrophils in cancer: Two sides of the same coin. *J Immunol Res* (2015) 2015:983698. doi: 10.1155/2015/983698
9. Papayannopoulos V. Neutrophil extracellular traps in immunity and disease. *Nat Rev Immunol* (2018) 18:134–47. doi: 10.1038/nri.2017.105
10. Dalbeth N, Gosling AL, Gaffo A, Abhishek A, Gout. *Lancet* (2021) 397:1843–55. doi: 10.1016/S0140-6736(21)00569-9
11. Josefs T, Barrett TJ, Brown EJ, Quezada A, Wu X, Voisin M, et al. Neutrophil extracellular traps promote macrophage inflammation and impair atherosclerosis resolution in diabetic mice. *JCI Insight* (2020) 5(7):e134796. doi: 10.1172/jci.insight.134796
12. Lee KH, Kronbichler A, Park DD, Park Y, Moon H, Kim H, et al. Neutrophil extracellular traps (NETs) in autoimmune diseases: A comprehensive review. *Autoimmun Rev* (2017) 16:1160–73. doi: 10.1016/j.autrev.2017.09.012
13. Veras FP, Pontelli MC, Silva CM, Toller-Kawahisa JE, de Lima M, Nascimento DC, et al. SARS-CoV-2-triggered neutrophil extracellular traps mediate COVID-19 pathology. *J Exp Med* (2020) 217(12):e20201129. doi: 10.1084/jem.20201129
14. Yang D, Liu J. Neutrophil extracellular traps: A new player in cancer metastasis and therapeutic target. *J Exp Clin Cancer Res* (2021) 40:233. doi: 10.1186/s13046-021-02013-6
15. Schedel F, Mayer-Hain S, Pappelbaum KI, Metzke D, Stock M, Goerge T, et al. Evidence and impact of neutrophil extracellular traps in malignant melanoma. *Pigment Cell Melanoma Res* (2020) 33:63–73. doi: 10.1111/pcmr.12818
16. Peng Z, Liu C, Victor AR, Cao DY, Veiras LC, Bernstein EA, et al. Tumors exploit CXCR4(hi)CD62L(lo) aged neutrophils to facilitate metastatic spread. *Oncoimmunology* (2021) 10:1870811. doi: 10.1080/2162402X.2020.1870811
17. Yang CH, Wang Z, Li LL, Zhang ZG, Jin X, Wu P, et al. Aged neutrophils form mitochondria-dependent vital NETs to promote breast cancer lung metastasis. *J Immunother Cancer* (2021) 9(10):e002875. doi: 10.1136/jitc-2021-002875
18. Mai J, Finley RL Jr., Waisman DM, Sloane BF. Human cathepsin b interacts with the annexin II tetramer on the surface of tumor cells. *J Biol Chem* (2000) 275:12806–12. doi: 10.1074/jbc.275.17.12806
19. Buck MR, Karustis DG, Day NA, Honn KV, Sloane BF. Degradation of extracellular-matrix proteins by human cathepsin b from normal and tumour tissues. *Biochem J* (1992) 282(Pt 1):273–8. doi: 10.1042/bj2820273
20. Campo E, Munoz J, Miquel R, Palacin A, Cardesa A, Sloane BF, et al. Cathepsin b expression in colorectal carcinomas correlates with tumor progression and shortened patient survival. *Am J Pathol* (1994) 145:301–9.
21. Zhang H, Fu T, McGettigan S, Kumar S, Liu S, Speicher D, et al. IL-8 and cathepsin b as melanoma serum biomarkers. *Int J Mol Sci* (2011) 12:1505–18. doi: 10.3390/ijms12031505
22. Sangster AB, Chang-McDonald B, Patel J, Bockett N, Paterson E, Davis PF, et al. Expression of cathepsins b and d by cancer stem cells in head and neck metastatic malignant melanoma. *Melanoma Res* (2021) 31:426–38. doi: 10.1097/CMR.0000000000000752
23. Campbell WC, Fisher MH, Stapley EO, Albers-Schonberg G, Jacob TA. Ivermectin: a potent new antiparasitic agent. *Science* (1983) 221:823–8. doi: 10.1126/science.6308762
24. Ashour DS. Ivermectin: From theory to clinical application. *Int J Antimicrob Agents* (2019) 54:134–42. doi: 10.1016/j.ijantimicag.2019.05.003
25. Tang M, Hu X, Wang Y, Yao X, Zhang W, Yu C, et al. Ivermectin, a potential anticancer drug derived from an antiparasitic drug. *Pharmacol Res* (2021) 163:105207. doi: 10.1016/j.phrs.2020.105207
26. Zhu M, Li Y, Zhou Z. Antibiotic ivermectin preferentially targets renal cancer through inducing mitochondrial dysfunction and oxidative damage. *Biochem Biophys Res Commun* (2017) 492:373–8. doi: 10.1016/j.bbrc.2017.08.097
27. Diao H, Cheng N, Zhao Y, Xu H, Dong H, Thamm DH, et al. Ivermectin inhibits canine mammary tumor growth by regulating cell cycle progression and WNT signaling. *BMC Vet Res* (2019) 15:276. doi: 10.1186/s12917-019-2026-2
28. Kraaij T, Tengstrom FC, Kamerling SW, Pusey CD, Scherer HU, Toes RE, et al. A novel method for high-throughput detection and quantification of neutrophil extracellular traps reveals ROS-independent NET release with immune complexes. *Autoimmun Rev* (2016) 15:577–84. doi: 10.1016/j.autrev.2016.02.018
29. Liu Z, Gu Y, Shin A, Zhang S, Ginhoux F. Analysis of myeloid cells in mouse tissues with flow cytometry. *STAR Protoc* (2020) 1:100029. doi: 10.1016/j.xpro.2020.100029
30. Guo F, Yang Z, Kulbe H, Albers AE, Sehoul J, Kaufmann AM. Inhibitory effect on ovarian cancer ALDH+ stem-like cells by disulfiram and copper treatment through ALDH and ROS modulation. *BioMed Pharmacother* (2019) 118:109371. doi: 10.1016/j.biopha.2019.109371
31. Hegde S, Leader AM, Merad M. MDSC: Markers, development, states, and unaddressed complexity. *Immunity* (2021) 54:875–84. doi: 10.1016/j.immuni.2021.04.004
32. Chen KW, Monteleone M, Boucher D, Sollberger G, Ramnath D, Condon ND, et al. Noncanonical inflammasome signaling elicits gasdermin d-dependent neutrophil extracellular traps. *Sci Immunol* (2018) 3(26):ear6676. doi: 10.1126/sciimmunol.aar6676
33. Sollberger G, Choidas A, Burn GL, Habenberger P, Lucrezia R, Kordes S, et al. Gasdermin d plays a vital role in the generation of neutrophil extracellular traps. *Sci Immunol* (2018) 3(26):ear6689. doi: 10.1126/sciimmunol.aar6689
34. Mulvihill E, Sborgi L, Mari SA, Pfreundschuh M, Hiller S, Muller DJ. Mechanism of membrane pore formation by human gasdermin-d. *EMBO J* (2018) 37(14):e9832137. doi: 10.15252/embj.201798321
35. Konreddy AK, Rani GU, Lee K, Choi Y. Recent drug-Repurposing-Driven advances in the discovery of novel antibiotics. *Curr Med Chem* (2019) 26:5363–88. doi: 10.2174/0929867325666180706101404
36. Hernandez JJ, Pryszlak M, Smith L, Yanchus C, Kurji N, Shahani VM, et al. Giving drugs a second chance: Overcoming regulatory and financial hurdles in repurposing approved drugs as cancer therapeutics. *Front Oncol* (2017) 7:273. doi: 10.3389/fonc.2017.00273
37. Jandova J, Park SL, Corenblum MJ, Madhavan L, Snell JA, Rounds L, et al. Mefloquine induces ER stress and apoptosis in BRAFi-resistant A375-BRAF (V600E) /NRAS(Q61K) malignant melanoma cells targeting intracranial tumors in a bioluminescent murine model. *Mol Carcinog* (2022) 61(6): 603–614. doi: 10.1002/mc.23407
38. Zhu L, Yang Q, Hu R, Li Y, Peng Y, Liu H, et al. Novel therapeutic strategy for melanoma based on albendazole and the CDK4/6 inhibitor palbociclib. *Sci Rep* (2022) 12:5706. doi: 10.1038/s41598-022-09592-0
39. Bista R, Lee DW, Pepper OB, Azorsa DO, Arcenci RJ, Aleem E. Disulfiram overcomes bortezomib and cytarabine resistance in down-syndrome-associated acute myeloid leukemia cells. *J Exp Clin Cancer Res* (2017) 36:22. doi: 10.1186/s13046-017-0493-5
40. Csoka B, Nemeth ZH, Szabo I, Davies DL, Varga ZV, Paloczi J, et al. Macrophage P2X4 receptors augment bacterial killing and protect against sepsis. *JCI Insight* (2018) 3(11):99431. doi: 10.1172/jci.insight.99431
41. Marcheva B, Weidemann BJ, Taguchi A, Perelis M, Ramsey KM, Newman MV, et al. P2Y1 purinergic receptor identified as a diabetes target in a small-molecule screen to reverse circadian beta-cell failure. *Elife* (2022) 11. doi: 10.7554/eLife.75132
42. Melotti A, Mas C, Kuciak M, Lorente-Trigos A, Borges I, Altares ARI. The river blindness drug ivermectin and related macrocyclic lactones inhibit WNT-TCF pathway responses in human cancer. *EMBO Mol Med* (2014) 6:1263–78. doi: 10.15252/emmm.201404084
43. Jiang L, Wang P, Sun YJ, Wu YJ. Ivermectin reverses the drug resistance in cancer cells through EGFR/ERK/Akt/NF-kappaB pathway. *J Exp Clin Cancer Res* (2019) 38:265. doi: 10.1186/s13046-019-1251-7
44. Azimi F, Scolyer RA, Rumcheva P, Moncrieff M, Murali R, McCarthy SW, et al. Tumor-infiltrating lymphocyte grade is an independent predictor of sentinel lymph node status and survival in patients with cutaneous melanoma. *J Clin Oncol* (2012) 30:2678–83. doi: 10.1200/JCO.2011.37.8539
45. Kluger HM, Zito CR, Barr ML, Baine MK, Chiang VL, Sznol M, et al. Characterization of PD-L1 expression and associated T-cell infiltrates in metastatic melanoma samples from variable anatomic sites. *Clin Cancer Res* (2015) 21:3052–60. doi: 10.1158/1078-0432.CCR-14-3073
46. Larkin J, Chiarion-Sileni V, Gonzalez R, Grob JJ, Rutkowski P, Lao CD, et al. Five-year survival with combined nivolumab and ipilimumab in advanced melanoma. *N Engl J Med* (2019) 381:1535–46. doi: 10.1056/NEJMoa1910836
47. Veglia F, Sanseviero E, Gabrilovich DI. Myeloid-derived suppressor cells in the era of increasing myeloid cell diversity. *Nat Rev Immunol* (2021) 21:485–98. doi: 10.1038/s41577-020-00490-y
48. Gabrilovich DI, Nagaraj S. Myeloid-derived suppressor cells as regulators of the immune system. *Nat Rev Immunol* (2009) 9:162–74. doi: 10.1038/nri2506
49. Kayagaki N, Stowe IB, Lee BL, O'Rourke K, Anderson K, Warming S, et al. Caspase-11 cleaves gasdermin d for non-canonical inflammasome signalling. *Nature* (2015) 526:666–71. doi: 10.1038/nature15541
50. Matikainen S, Nyman TA, Cypriak W. Function and regulation of noncanonical caspase-4/5/11 inflammasome. *J Immunol* (2020) 204:3063–9. doi: 10.4049/jimmunol.2000373
51. Gao W, Li Y, Liu X, Wang S, Mei P, Chen Z, et al. TRIM21 regulates pyroptotic cell death by promoting gasdermin d oligomerization. *Cell Death Differentiation* (2022) 29:439–50. doi: 10.1038/s41418-021-00867-z
52. Kambara H, Liu F, Zhang X, Liu P, Bajrami B, Teng Y, et al. Gasdermin d exerts anti-inflammatory effects by promoting neutrophil death. *Cell Rep* (2018) 22:2924–36. doi: 10.1016/j.celrep.2018.02.067
53. Burgener SS, Leborgne NGF, Snipas SJ, Salvesen GS, Bird PI, Benarafa C. Cathepsin G inhibition by Serpinb1 and Serpinb6 prevents programmed necrosis

in neutrophils and monocytes and reduces GSDMD-driven inflammation. *Cell Rep* (2019) 27:3646–56.e3645. doi: 10.1016/j.celrep.2019.05.065

54. Xia H, Qin M, Wang Z, Wang Y, Chen B, Wan F, et al. A pH-/Enzyme-Responsive nanoparticle selectively targets endosomal toll-like receptors to potentiate robust cancer vaccination. *Nano Lett* (2022) 22:2978–87. doi: 10.1021/acs.nanolett.2c00185

55. Li X, Liang Y, Lian C, Peng F, Xiao Y, He Y, et al. CST6 protein and peptides inhibit breast cancer bone metastasis by suppressing CTSB activity and osteoclastogenesis. *Theranostics* (2021) 11:9821–32. doi: 10.7150/thno.62187

56. Bromme D, Okamoto K, Wang BB, Biroc S. Human cathepsin O2, a matrix protein-degrading cysteine protease expressed in osteoclasts. functional expression of human cathepsin O2 in *Spodoptera frugiperda* and characterization of the enzyme. *J Biol Chem* (1996) 271:2126–32. doi: 10.1074/jbc.271.4.2126

57. Tjaderhane L, Nascimento FD, Breschi L, Mazzoni A, Tersariol IL, Geraldeli S, et al. Optimizing dentin bond durability: control of collagen degradation by matrix metalloproteinases and cysteine cathepsins. *Dent Mater* (2013) 29:116–35. doi: 10.1016/j.dental.2012.08.004

58. Tripathi R, Fiore LS, Richards DL, Yang Y, Liu J, Wang C, et al. Abl and arg mediate cysteine cathepsin secretion to facilitate melanoma

invasion and metastasis. *Sci Signal* (2018) 11(518):eaao0422. doi: 10.1126/scisignal.aao0422

59. Chevriaux A, Pilot T, Derangere V, Simonin H, Martine P, Chalmin F, et al. Cathepsin b is required for NLRP3 inflammasome activation in macrophages, through NLRP3 interaction. *Front Cell Dev Biol* (2020) 8:167. doi: 10.3389/fcell.2020.00167

60. Richmond A, Yang J, Su Y. The good and the bad of chemokines/chemokine receptors in melanoma. *Pigment Cell Melanoma Res* (2009) 22:175–86. doi: 10.1111/j.1755-148X.2009.00554.x

61. Moretti S, Pinzi C, Spallanzani A, Berti E, Chiarugi A, Mazzoli S, et al. Immunohistochemical evidence of cytokine networks during progression of human melanocytic lesions. *Int J Cancer* (1999) 84:160–8. doi: 10.1002/(SICI)1097-0215(19990420)84:2<160::AID-IJC12>3.0.CO;2-R

62. Rossi S, Cordella M, Tabolacci C, Nassa G, D'Arcangelo D, Senatore C, et al. TNF-alpha and metalloproteases as key players in melanoma cells aggressiveness. *J Exp Clin Cancer Res* (2018) 37:326. doi: 10.1186/s13046-018-0982-1

63. Bertrand F, Montfort A, Marcheteau E, Imbert C, Gilhodes J, Filleron T, et al. TNFalpha blockade overcomes resistance to anti-PD-1 in experimental melanoma. *Nat Commun* (2017) 8:2256. doi: 10.1038/s41467-017-02358-7